Iskandar et al.:

3-D Nasal Cultures: Systems Toxicological Assessment of a Candidate Modified-Risk Tobacco Product

Supplementary Data

Supplementary materials and methods

Normalization of the adenylate kinase (AK)-based cytotoxicity assay

For each of the five experimental repetitions, the value of the luminescence signal was normalized using the mean of the positive control (Cultures treated with 1% Triton X-100 for 24 h; considered as 100% cytotoxicity) and negative control (PBS-treated or untreated cultures; considered as 0% cytotoxicity):

Formula S1

$$Cytotoxicity\ (\%) = \frac{AK_{Tissue} - AK_{Neg\ CTRL}}{AK_{Pos\ CTRL} - AK_{Neg\ CTRL}}\ x\ 100, \text{ where}$$

$$AK_{Pos\ CTRL} = \sum_{i=1}^{nbPhase} \frac{AK_{TX-100}}{nbPhase}$$

$$AK_{Neg\ CTRL} = \sum_{i=1}^{nbPhase} \frac{\sum_{j=1}^{nbCTRL^i} \frac{AK_{i,j}}{nbCTRL^i}}{nbPhase}$$

$$AK_{Tissue} = relative\ luminescence\ unit\ of\ a\ given\ sample$$
$$nbPhase = number\ of\ experimental\ phase$$

$$Neg = negative$$

$$Pos = positive$$

$$CTRL = control$$

The averages of the normalized relative luminescence unit were reported.

Normalization of the cytochrome P450 activity assay

For each of the five experimental repetitions, the CYP1A1/1B1 activity levels were reported relative to the luminescence signals of the mean of triplicate positive controls (tissue inserts treated with 30 nM TCDD for 48 were considered 100% activity induction) and negative controls (luciferin-CEE (substrate only)-treated cultures considered as 0% activity):

Formula S2

$$Normalized\ CYP\ activity\ (\%) = \frac{CYP_{Tissue} - CYP_{Neg\ CTRL}}{CYP_{Pos\ CTRL} - CYP_{Neg\ CTRL}}\ x\ 100, \text{ where}$$

$$CYP_{Neg\ CTRL} = \sum_{i=1}^{nbPhase} \frac{\sum_{j=1}^{nbCTRL^i} \frac{CYP_{i,j}}{nbCTRL^i}}{nbPhase}$$

$$CYP_{Pos\ CTRL} = \sum_{i=1}^{nbPhase} \frac{CYP_{TCDD}}{nbPhase}$$

$$CYP_{Tissue} = relative\ luminescence\ unit\ of\ a\ given\ tissue\ culture\ sample$$
$$nbPhase = number\ of\ experimental\ phase$$

$$Neg = negative$$

$$Pos = positive$$

$$CTRL = control$$

Normalization of the FFT power to calculate the power of the detected signal of cilia beating

The FFT power was normalized to the ambient noise using the following formula:

Formula S3

$$\frac{'T\ Magnitude - \ Lowest\ FFT\ Magnitude^2}{Lowest\ FFT\ Magnitude}$$

$$FFT = \text{Fast Fourier Transformation}$$

https://doi.org/10.14573/altex.1605041s

Supplementary figures

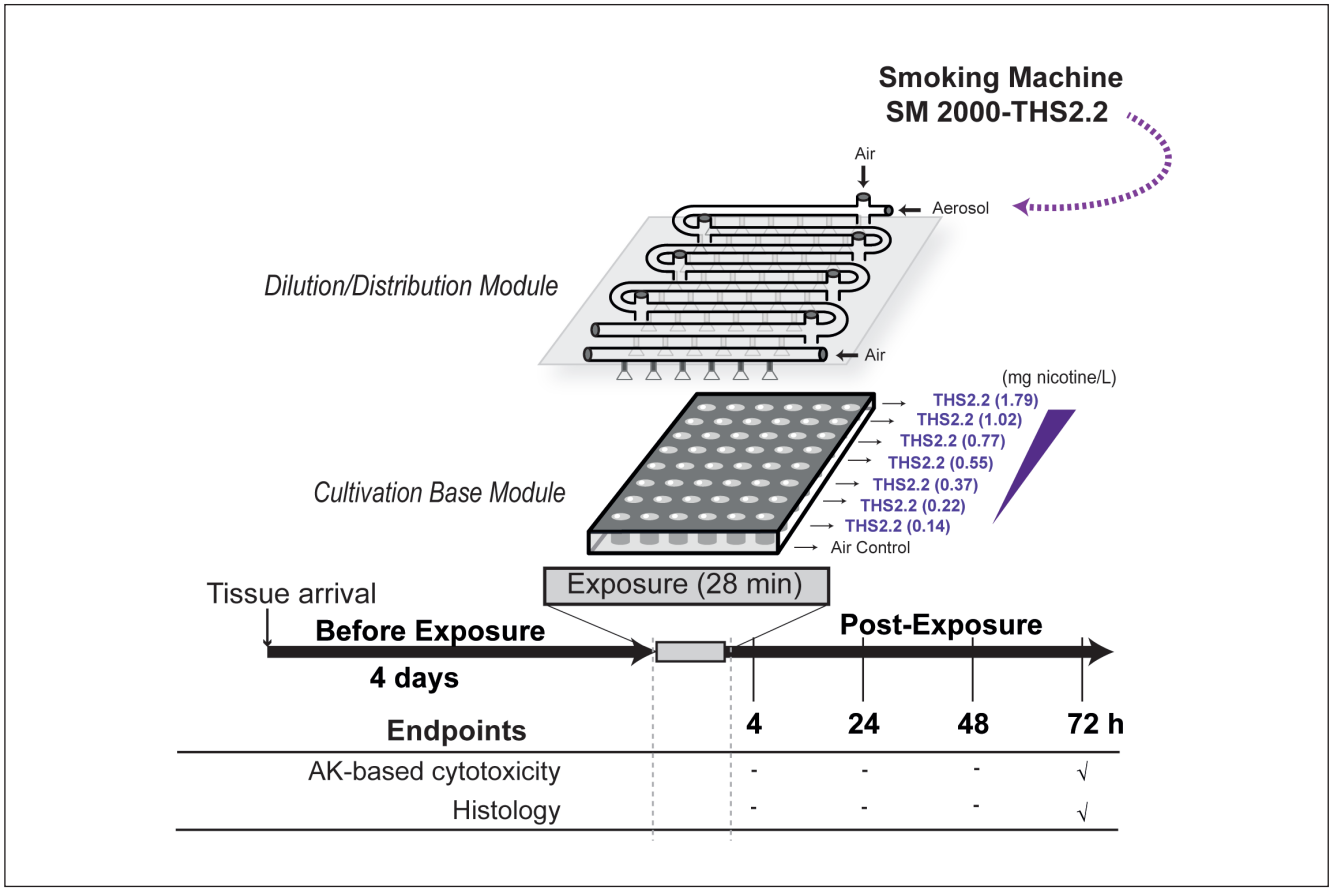

Fig. S1: Exposure run and endpoint schematic for the dose range assessment of THS2.2 aerosol
Tissue cultures were exposed to THS2.2 aerosols at the apical side using the Vitrocell® 24/48 exposure system connected to the smoking machine (SM) 2000-THS2.2. The system has a Dilution/Distribution Module where dilutions of THS2.2 aerosol were applied to reach the target nicotine concentrations in the THS2.2 aerosol. The numbers in parentheses indicate the concentration of nicotine in the THS2.2 aerosol (mg/l). For each group, cytotoxicity and histological analyses were measured at 72 h post-exposure.

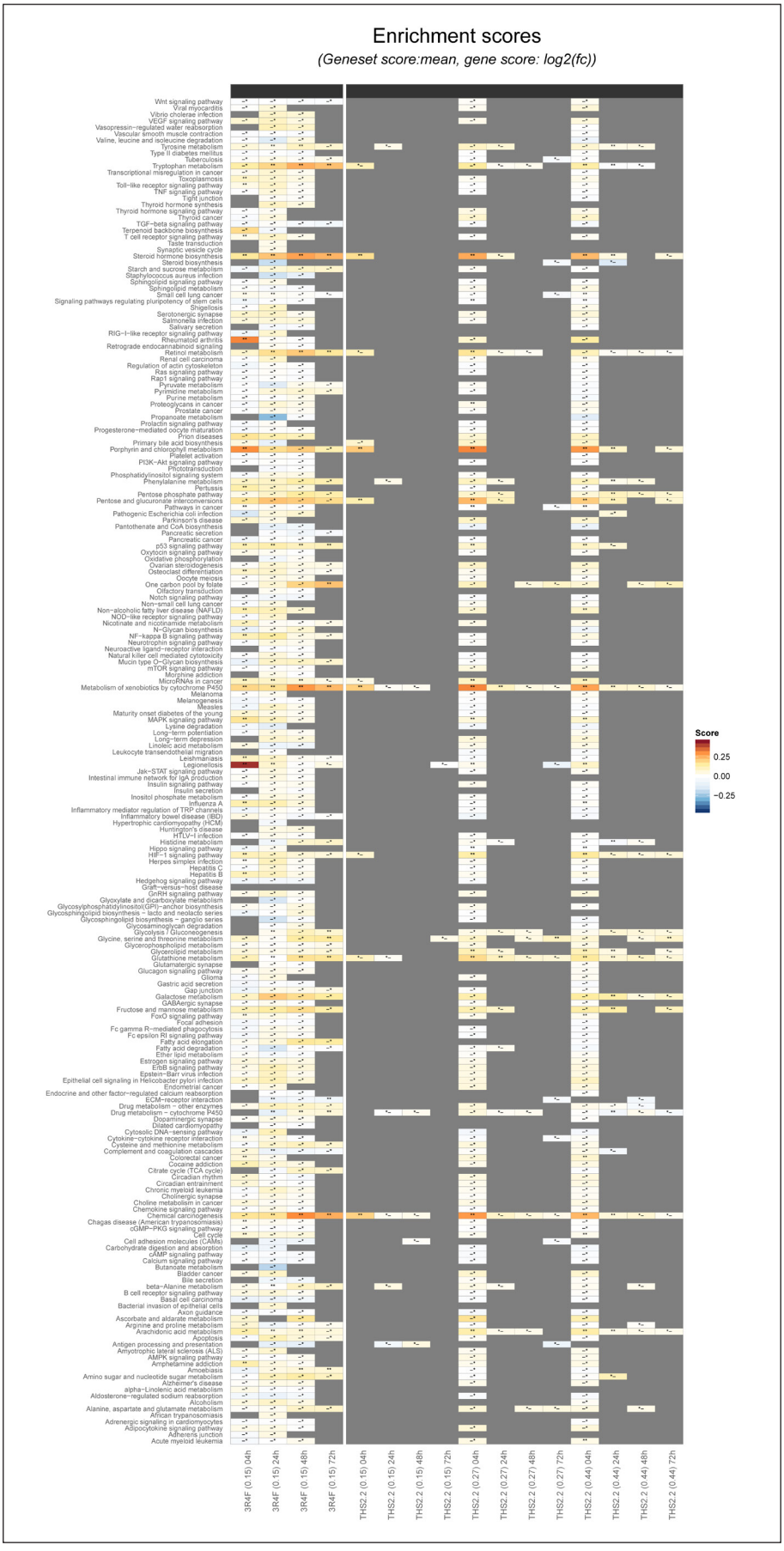

Fig. S2: Gene-set analysis showing various biological pathways enriched in the datasets

A heatmap showing all KEGG pathways that were significantly enriched in t he dataset. The color gradient represents the score enrichment: the mean of the gene score (log_2(fold-change)). Two categories of significance are shown: first and second characters indicate Q1 and Q2, respectively.

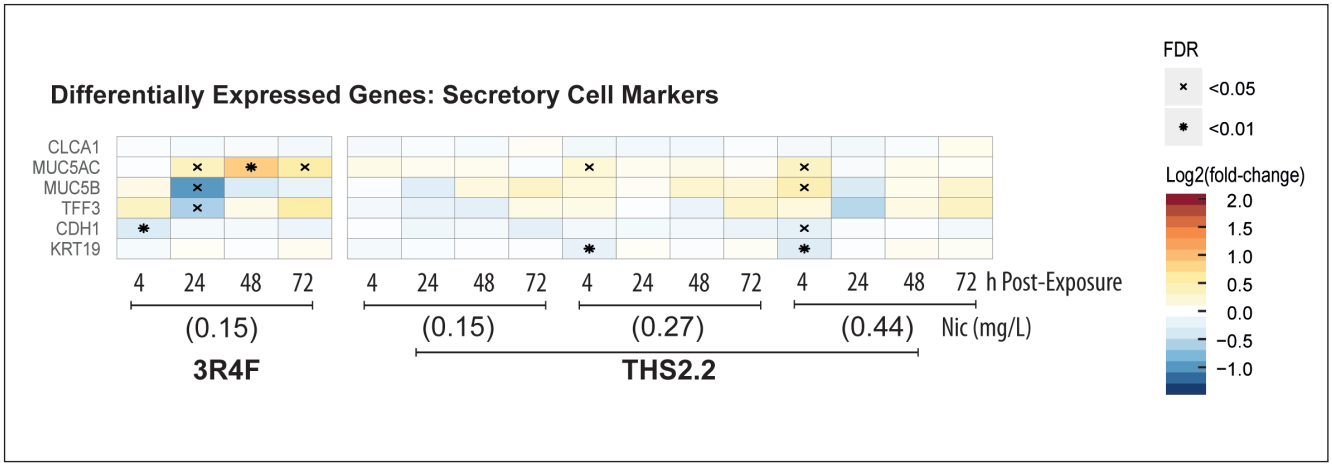

Fig. S3: Impact of exposures on cellular markers of secretory cells
The heatmap represents the levels of gene expression changes (log_2 of the fold-changes) that were significantly impacted by exposure when compared with their respective air controls. The list of genes was compiled based on previously reported findings in: (Hupin et al., 2014; Noruddin et al., 2007; Brezillon et al., 1995; LeSimple et al., 2007; Raiford et al., 2011; Schlage et al., 1998; Jiao et al., 2015). The gene names are listed on the left side of the heatmap.

References:

Hupin, C., Gohy, S., Bouzin, C. et al. (2014). Features of mesenchymal transition in the airway epithelium from chronic rhinosinusitis. *Allergy 69*, 1540-1549. https://doi.org/10.1111/all.12503

Noruddin, N. A., Saim, A. B., Chua, K. H. et al. (2007). Human nasal turbinates as a viable source of respiratory epithelial cells using co-culture system versus dispase-dissociation technique. *Laryngoscope 117*, 2139-2145. https://doi.org/10.1097/MLG.0b013e3181453a1e

Brezillon, S., Dupuit, F., Hinnrasky, J. et al. (1995). Decreased expression of the CFTR protein in remodeled human nasal epithelium from non-cystic fibrosis patients. *Lab Invest 72*, 191-200. https://doi.org/10.1371/journal.pone.0057617

LeSimple, P., van Seuningen, I., Buisine, M. P. et al. (2007). Trefoil factor family 3 peptide promotes human airway epithelial ciliated cell differentiation. *Am J Respir Cell Mol Biol 36*, 296-303. https://doi.org/10.1165/rcmb.2006-0270OC

Raiford, K. L., Park, J., Lin, K.-W. et al. (2011). Mucin granule-associated proteins in human bronchial epithelial cells: The airway goblet cell "granulome". *Respir Res 12*, 1-10. https://doi.org/10.1186/1465-9921-12-118

Schlage, W. K., Bulles, H., Friedrichs, D. et al. (1998). Cytokeratin expression patterns in the rat respiratory tract as markers of epithelial differentiation in inhalation toxicology. I. Determination of normal cytokeratin expression patterns in nose, larynx, trachea, and lung. *Toxicol Pathol 26*, 324-343. https://doi.org/10.1177/019262339802600307

Jiao, J., Duan, S., Meng, N. et al. (2015). Role of IFN-gamma, IL-13 and IL-17 on mucociliary differentiation of nasal epithelial cells in chronic rhinosinusitis with nasal polyps. *Clin Exp Allergy 46*, 449-460. https://doi.org/10.1111/cea.12644

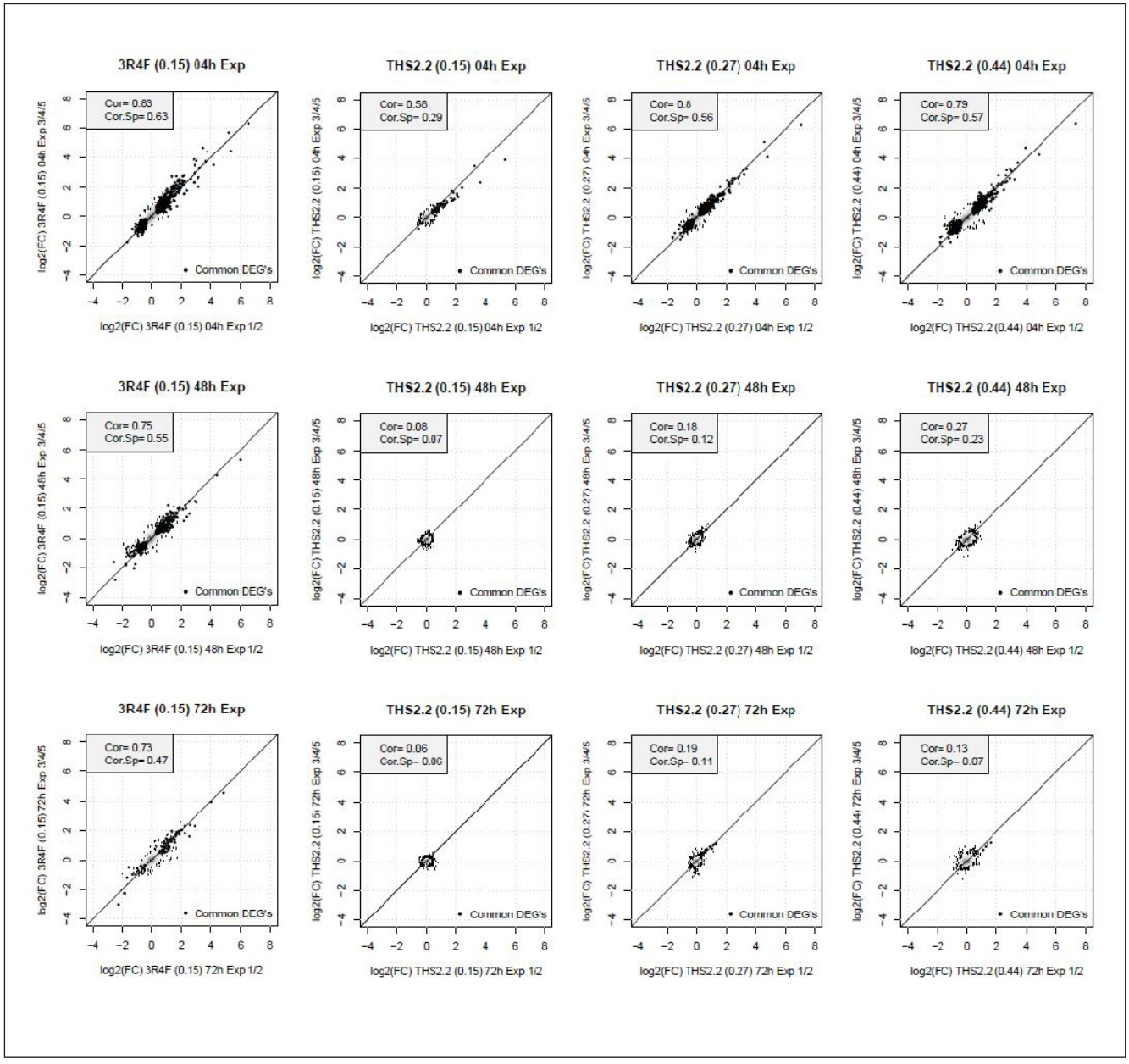

Fig. S4: Correlation plots of gene fold-changes generated from the microarray analysis

Each dot represents a gene. The fold-change of a given gene from the combined experiments 1 and 2 (x-axis) was compared with the fold-change of the same gene from the combined experiment 3, 4, and 5 (y-axis).

Abbreviations: Corr, correlation; Sp, Spearman correlation; DEG, differentially expressed gene.

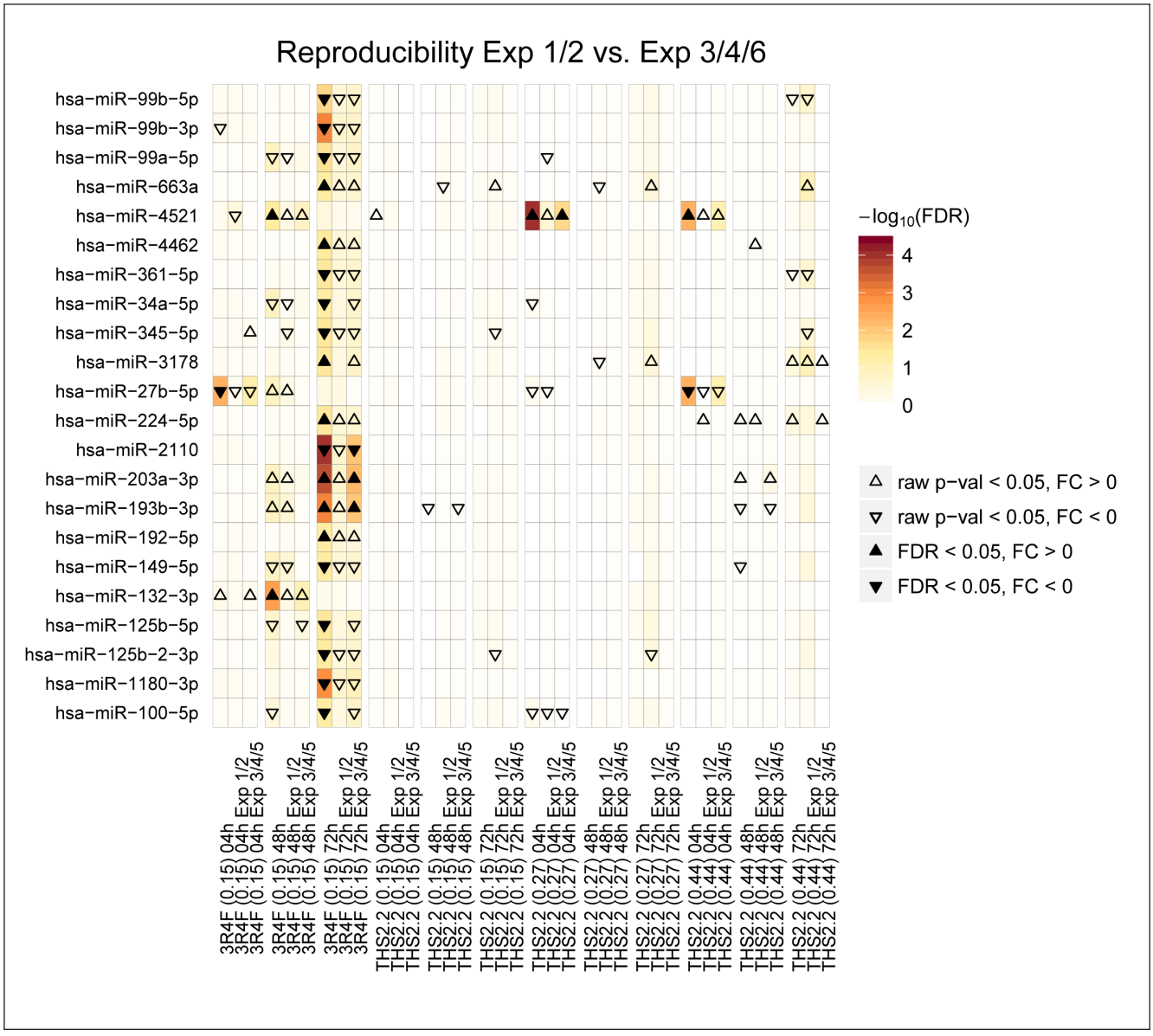

Fig. S5: Comparability of miRNA fold-changes generated across the experimental repetitions
The miRNAs are listed on the left side of the heatmap. Each exposure condition (and post-exposure time-point) comprised three columns: first, combined data from experimental repetition 1/2/3/4/5; second, combined data from experimental repetition 1/2; and combined data from experimental 3/4/5. The color gradation indicates the level of the differentially expressed miRNA (-$\log_{10}$(FDR). The △ and ▽ signs indicate increased and decreased expression levels, respectively.
Abbreviations: Exp, experiment; FC, fold-change; FDR, false discovery rate; hsa, homo sapiens.

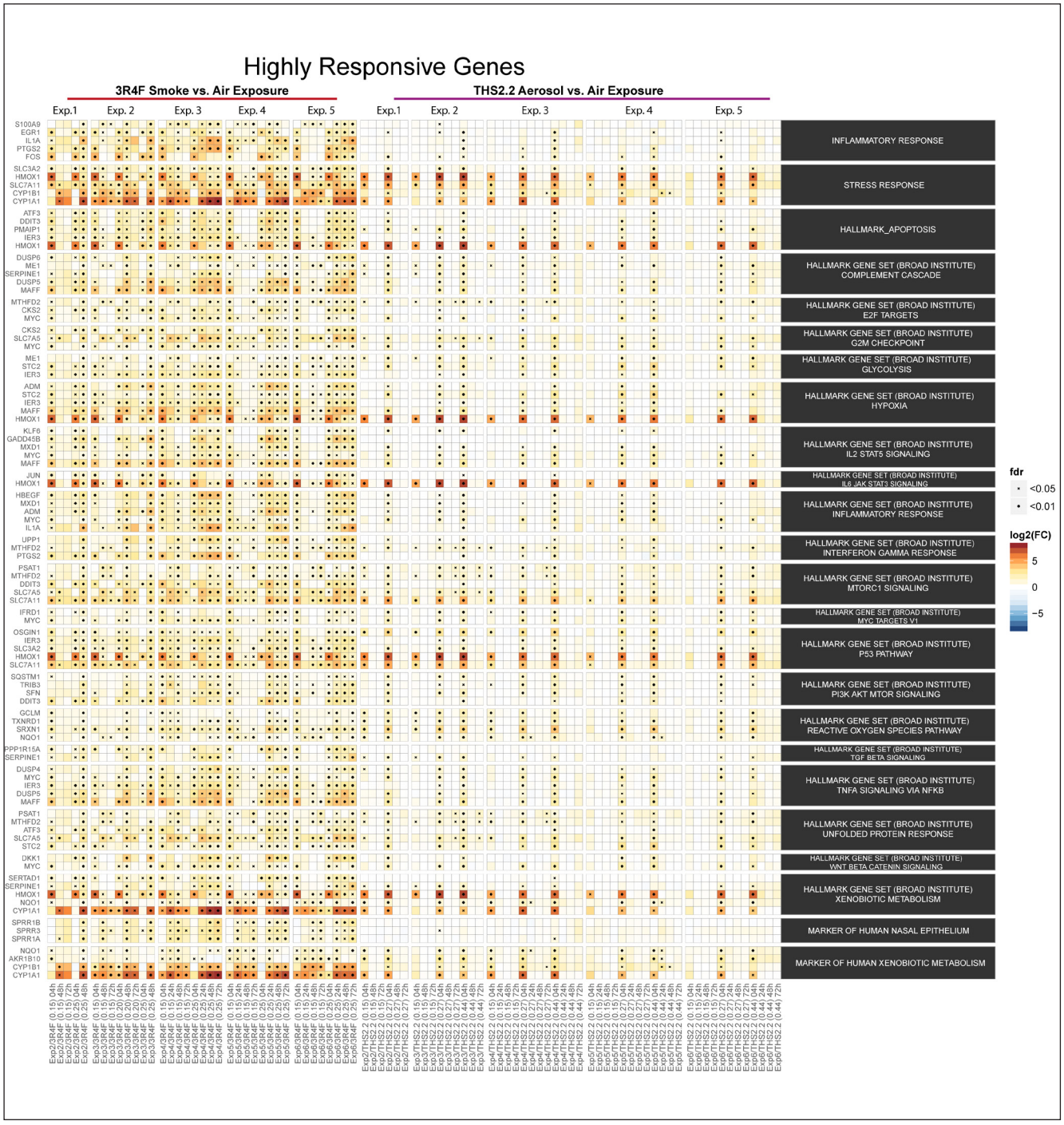

Fig. S6: Highly responsive genes consistently observed across the experimental repetitions

The list of genes is provided as an example from which a gene panel can be developed and used in future studies. From each of the experimental repetitions (Exp.), for all exposure conditions and post-exposure time points, highly responsive genes were chosen if they: i) were present in at least 20% of all comparisons (listed at the bottom of the heatmap); ii) had FDR < 0.05 and absolute $\log_2$(fold-change) > 1; and iii) the mean expression levels ($\log_2$(FRMA value)) in the air control and exposed groups were both > 4. A total of 49 genes are present in the heatmap (they belong to multiple processes listed on the right side of the heatmap): *ADM, AKR1B10, ATF3, CKS2, CYP1A1, CYP1B1, DDIT3, DKK1, DUSP4, DUSP5, DUSP6, EGR1, GADD4B, GCLM, HBEGF, HMOX1, IER3, IFRD1, IL1A, JUN, KLF6, MAFF, ME1, MTHFD2, MXD1, MYC, NQO, NQO1, OSGIN1, PMAIP1, PPP1R1A, PSAT1, PTGS2, S100A9, SERPINE1, SERTAD1, SFN, SLC3A2, SLC7A11, SLC7A5, SPRR1A, SPRR1B, SPRR3, SQSTM1, SRXN1, STC2, TRIB3, XNRD1, UPP1*. The multiple processes are taken from the hallmark gene sets (Broad Institute) and gene sets developed by our group.

Tab. S1: Sample number

Collection Time	Group	Total sample number per endpoint					
		AK-based cytotoxicity	CYP1A1/1B1 activity	Secretion of Mediators	Histology/immunostaining	Ciliary beating frequency	mRNA and miRNA profiles
Before	3R4F (Air)	-	-	-	-	9	-
	3R4F (0.15)	-	-	-	-	9	-
	3R4F (0.25)	-	-	-	-	9	-
	THS2.2 (Air)	-	-	-	-	9	-
	THS2.2 (0.15)	-	-	-	-	9	-
	THS2.2 (0.27)	-	-	-	-	9	-
	THS2.2 (0.44)	-	-	-	-	9	-
0h PE	3R4F (Air)	-	-	-	-	9	-
	3R4F (0.15)	-	-	-	-	9	-
	3R4F (0.25)	-	-	-	-	9	-
	THS2.2 (Air)	-	-	-	-	9	-
	THS2.2 (0.15)	-	-	-	-	9	-
	THS2.2 (0.27)	-	-	-	-	9	-
	THS2.2 (0.44)	-	-	-	-	9	-
4 h PE	3R4F (Air)	15	-	-	-	-	14
	3R4F (0.15)	15	-	-	-	-	15
	3R4F (0.25)	15	-	-	-	-	-
	THS2.2 (Air)	15	-	-	-	-	15
	THS2.2 (0.15)	15	-	-	-	-	15
	THS2.2 (0.27)	15	-	-	-	-	15
	THS2.2 (0.44)	12	-	-	-	-	12
24 h PE	3R4F (Air)	9	6	9	-	9	9
	3R4F (0.15)	9	6	9	-	9	9
	3R4F (0.25)	9	6	9	-	9	-
	THS2.2 (Air)	9	6	9	-	9	9
	THS2.2 (0.15)	9	6	9	-	9	9
	THS2.2 (0.27)	9	6	9	-	9	9
	THS2.2 (0.44)	9	3	9	-	9	9
48 h PE	3R4F (Air)	15	15	15	15	9	14
	3R4F (0.15)	15	15	15	14	9	15
	3R4F (0.25)	15	15	15	-	9	-
	THS2.2 (Air)	15	15	15	15	9	14
	THS2.2 (0.15)	15	15	15	15	9	14
	THS2.2 (0.27)	15	15	15	15	9	15
	THS2.2 (0.44)	12	12	12	12	9	12
72 h PE	3R4F (Air)	15	6	9	15	-	14
	3R4F (0.15)	15	6	9	15	-	15
	3R4F (0.25)	15	6	9	-	-	-
	THS2.2 (Air)	15	6	9	15	-	14
	THS2.2 (0.15)	15	6	9	15	-	15
	THS2.2 (0.27)	15	6	9	15	-	15
	THS2.2 (0.44)	12	3	9	12	-	12
72 h PE – Dose Range Assessment	THS2.2 (Air)	3	-	-	3	-	-
	THS2.2 (0.14)	3	-	-	2	-	-
	THS2.2 (0.22)	3	-	-	3	-	-
	THS2.2 (0.37)	3	-	-	3	-	-
	THS2.2 (0.55)	3	-	-	3	-	-
	THS2.2 (0.77)	3	-	-	3	-	-
	THS2.2 (1.02)	3	-	-	3	-	-
	THS2.2 (1.79)	3	-	-	3	-	-

Abbreviations: AK, adenylate kinase; CYP, cytochrome P450; PE, post-exposure; THS, tobacco heating system

Tab. S2: List of network models considered in the study

Number	Abbreviated network family name	Network name
1	CFA	Apoptosis
2	CFA	Autophagy
3	CFA	Necroptosis
4	CFA	Response To DNA Damage
5	CFA	Senescence
6	CPR	Calcium
7	CPR	Cell Cycle
8	CPR	Cell Interaction
9	CPR	Clock
10	CPR	Epigenetics
11	CPR	Growth Factor
12	CPR	Hedgehog
13	CPR	Hox
14	CPR	Jak Stat
15	CPR	Mapk
16	CPR	Mtor
17	CPR	Notch
18	CPR	Nuclear Receptors
19	CPR	PGE2
20	CPR	Wnt
21	CST	Endoplasmic Reticulum Stress
22	CST	Hypoxic Stress
23	CST	NFE2L2 Signaling
24	CST	Osmotic Stress
25	CST	Oxidative Stress
26	CST	Xenobiotic Metabolism Response
27	IPN	Epithelial Innate Immune Activation
28	IPN	Epithelial Mucus Hypersecretion
29	IPN	Tissue Damage

Abbreviations: CFA, Cell Fate; CST, Cell Stress; CPR, Cell Proliferation; IPN, Inflammatory Process Networks; Jak Stat, janus kinase/signal transducers and activators of transcription; Mapk, mitogen-activated protein kinases; Mtor, mechanistic target of rapamycin; NFE2l2, nuclear factor, erythroid 2-like 2; PGE2, prostaglandin E2. The collection of causal biological networks used in the study(s) was the human network suite CBN v1.3 (Boué et al., 2015).

Tab. S3: Potential target mRNA per miRNA cluster

Cluster a	Cluster b	Cluster c	Cluster d
MLF2	CENPQ	SEMA7A	DDX5
KDELR1	TNRC6B	NEK11	H2AFV
SCRIB	RALGDS	SMPD2	EFEMP1
INPPL1	PBXIP1	KDM2A	SRSF6
NPDC1	ZNF652	SYMPK	VPS13C
SBNO2	ZNF789	GDAP2	MYCN
HYOU1		KIF9	TMF1
HMGA1		BAG3	HNMT
CCDC71L		JUN	ANKH
MARK4		PARK7	NET1
SLC25A3		ERCC3	SEPW1
DLGAP4		HSPA1A	RUVBL1
METRNL		FNIP2	CCP110
CAP1		DNAJA1	SH3BP5
TROVE2		WWTR1	SUN1
NFE2L2		ARHGEF4	ENAH
PVRL4		CCP110	RMI1
OSTF1		DUSP22	ATP1A1
TMBIM1		ST3GAL1	MYLK
PROM2		PLD4	PSIP1
EFHD2		SEMA4D	LEF1
PDP1		ARHGAP21	SNRK
EPRS		E2F3	EPDR1
ESYT1		MAP1B	EFHD1
MARCKSL1		SBNO1	CEP128
SHMT2		ZNF281	FOXP2
SBF1		RC3H1	FZD6
PPP4C		UBAP2	AZIN1
GPI		PER2	CD164
MAN2A1		YPEL5	SH3RF3
SSR2		MARCH6	PECR

Cluster a	Cluster b	Cluster c	Cluster d
SDC1		PREX1	SYNM
RFC2		CUX1	CAPS2
TRIP6		FOXN2	WDR35
ESPL1		ARHGAP30	TNC
KIF1C		ZNF44	RBM5
RAP1GAP2		KIAA0753	CYSTM1
ARPC2		KIAA0040	DSTN
TNPO3		JUNB	DNAJA4
LRRC41		IQCB1	STXBP4
NAT10		GTF2E2	B2M
BIRC5			SMAD4
GAPDH			EYA4
YWHAE			NEDD4L
TKT			SLC7A2
TRIM28			DDX6
OPTC			ARRDC3
RER1			LIFR
CNN2			SPARC
WDR41			PCNXL4
EXT1			ABI3BP
NOP9			PPAP2B
SESN2			NBEA
TTC39A			C12orf75
ATXN2L			ID4
INO80D			
AP2B1			
RARS			
PABPC4			
TIAM1			
BICD2			
MRPL10			

Tab. S4: Enrichment analysis of the miRNA target genes using EnrichR

KEGG pathway	Cluster	Number of overlap genes in the pathway	Genes	EnrichR's combined score	KEGG pathway class
Aminoacyl trna biosynthesis	a	2/38	RARS;EPRS	3.2081542	Translation
Arginine and proline metabolism	a	2/34	RARS;EPRS	3.1812275	Amino acid metabolism
Glycolysis and gluconeogenesis	a	2/63	GPI;GAPDH	2.687253	Carbohydrate metabolism
Cell cycle	a	2/104	YWHAE;ESPL1	2.1183877	Cell growth and death
Glycan structures biosynthesis 1*	a	2/106	EXT1;MAN2A1	2.0471369	Glycan biosynthesis and metabolism
Pancreatic cancer	b	1/73	RALGDS	7.7656622	(Excluded because of disease specific)
Colorectal cancer	b	1/84	RALGDS	7.4848943	(Excluded because of disease specific)
Axon guidance	c	2/126	SEMA7A;SEMA4D	1.8327301	Development
Glycosphingolipid biosynthesis globoseries	c	1/14	ST3GAL1	1.6650896	Glycan biosynthesis and metabolism
Circadian rhythm	c	1/11	PER2	1.6189169	Environmental adaptation
Glycosphingolipid biosynthesis ganglioseries	c	1/16	ST3GAL1	1.5454733	Glycan biosynthesis and metabolism
Keratan sulfate biosynthesis	c	1/16	ST3GAL1	1.3647478	Glycan biosynthesis and metabolism
Basal transcription factors	c	1/33	GTF2E2	1.1850813	Transcription
Sphingolipid metabolism	c	1/36	SMPD2	1.1546578	Lipid metabolism
Adherens junction	d	2/75	SMAD4;LEF1	3.8679593	Cellular community
Focal adhesion	d	2/192	TNC;MYLK	2.6127561	Cellular community
Ether lipid metabolism	d	1/30	PPAP2B	1.7928805	Lipid metabolism
Histidine metabolism	d	1/40	HNMT	1.7270358	Amino acid metabolism
Sphingolipid metabolism	d	1/36	PPAP2B	1.5076568	Lipid metabolism
Glycerolipid metabolism	d	1/55	PPAP2B	1.3500408	Lipid metabolism
Glycerophospholipid metabolism	d	1/62	PPAP2B	1.2795226	Lipid metabolism
Ecm receptor interaction	d	1/87	TNC	1.1061538	Signaling molecules and interaction
Polyunsaturated fatty acid biosynthesis	d	1/13	PECR	1.0066938	Lipid metabolism

* "Glycan structures-biosynthesis 1" is merged to KEGG Pathway 00510 "N-Glycan biosynthesis"
(see http://www.genome.jp/kegg/docs/upd_map.html)